Mechanics & Industry 14, 447–451 (2013)
© AFM, EDP Sciences 2014
DOI: 10.1051/meca/2013080
www.mechanics-industry.org

Mechanics & Industry

# Thermal effects of $CO_2$ capture by solid adsorbents: some approaches by IR image processing

J.F. Benevides Ferreira[1,2,3,a], C. Pradere[1], J. Jolly[3], G. Le Bourdon[2], J. Mascetti[2], B. Pavageau[3], L. Servant[2] and J.-C. Batsale[1]

[1] Laboratoire I2M-TREFLE, UMR 5295, Esplanade des Arts et Métiers, 33405 Talence Cedex, France
[2] ISM, UMR 5255, Université Bordeaux 1, 351 cours de la libération, 33405 Talence Cedex, France
[3] Solvay-Rhodia LOF, UMR 5258, 178 avenue du Docteur Schweitzer, 33608 Pessac Cedex, France

Received 26 June 2013, Accepted 19 November 2013

**Abstract –** Thanks to infrared thermography, we have studied the mechanisms of $CO_2$ capture by solid adsorbents ($CO_2$ capture via gas adsorption on various types of porous substrates) to better understand the physico-chemical mechanisms that control $CO_2$-surface interactions. In order to develop in the future an efficient process for post-combustion $CO_2$ capture, it is necessary to quantify the energy of adsorption of the gas on the adsorbent (exothermic process). The released heat (heat of adsorption) is a key parameter for the choice of materials and for the design of capture processes. Infrared thermography is used, at first approach, to detect the temperature fields on a thin-layer of adsorbent during $CO_2$ adsorption. An analytical heat transfer model was developed to evaluate the adsorption heat flux and to estimate, via an inverse technique, the heat of adsorption. The main originality of our method is to estimate heat losses directly from the heat generated during the adsorption process. Then, the estimated heat loss is taken for an a posteriori calculation of the adsorption heat flux. Finally, the heat of adsorption may be estimated. The interest in using infrared thermography is also its ability to quickly change the experimental setup, for example, to switch from the adsorbent thin-layer to the adsorbent bed configuration. We present the first results tempting to link the thin-layer data to the propagation speed of the thermal front in a millifluidics adsorption bed, also observed by IR thermography.

**Key words:** $CO_2$ adsorption / IR thermography / thermal model / heat of adsorption / inverse technique

## 1 Introduction

According to *the Climate Change 2007: Synthesis Report* [1] from the Intergovernmental Panel on Climate Change (IPCC), the greenhouse gas (GHG) emissions due to human activities have considerably grown since pre-industrial times. It was also found that carbon dioxide ($CO_2$) is the most important anthropogenic GHG, representing 77% of total GHG emissions. The largest growth in GHG emissions has come from energy supply, transport and industry. The report states that most of the observed increase in global average temperatures since the mid 20th century is very likely due to the observed increase in anthropogenic GHG concentrations. Extensive efforts have been devoted to reducing $CO_2$ emissions, especially to the development of $CO_2$ capture technologies [2]. $CO_2$ capture by solid adsorbents ($CO_2$ capture via gas adsorption on porous materials) is one of the most promising capture technology due to its high selectivity and low energy penalties [3]. The study of the physicochemical mechanisms that control $CO_2$-adsorbent interactions is essential when we are looking for efficient $CO_2$ capture concerning the adsorbent and the design of capture processes. The adsorption of a gas on an adsorbent is exothermic. The study of the energy released during the interaction $CO_2$-substrate (heat of adsorption), leads to a better understanding of these physicochemical mechanisms. The estimation of adsorption heats is thus crucial. A high heat of adsorption leads to a high $CO_2$-adsorbent interaction. This means that the material has a good affinity with the $CO_2$ molecules, allowing favorable $CO_2$ capture. However, energetic interactions may impede the material regeneration (desorption of $CO_2$ from adsorbent). Therefore, the heat of adsorption is a key parameter for the selection of materials. The heat of adsorption may be measured by calorimetric techniques [4] or estimated via adsorption isotherms [5]. Both methods are widely used, but high cost equipments and time-consuming experiments are necessary, hindering the use of high-throughput methodologies. In most adsorption processes, the adsorbent is in contact with fluid in a

[a] Corresponding author: jffbenev@yahoo.com.br

Article published by EDP Sciences

https://doi.org/10.1051/meca/2013080 Published online by Cambridge University Press

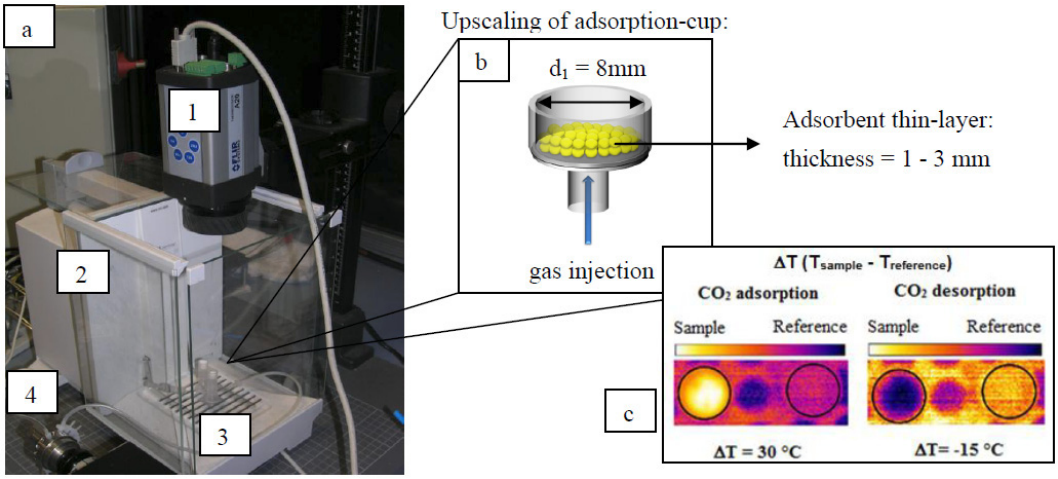



**Fig. 1.** (a) Experimental device. (b) Scheme of adsorption cup. (c) IR image of adsorption/desorption.

packed bed. The analysis and rational design of such processes therefore require an understanding of the dynamic behavior of such systems [6]. Until recently, many authors have utilized the simultaneous solution of a set of coupled nonlinear partial differential equations (PDEs) based on heat and mass balances to predict the adsorption column (adsorber) dynamics [7–9]. The balance equations take into account complex phenomena (e.g. diffusion, dispersion...) and many parameters have to be used as inputs in the model. Moreover, these parameters are hardly measured or estimated. A direct methodology is used by these authors, which consists in fitting experimental results (adsorbent temperature and gas-phase concentration) with the mentioned PDEs. The disadvantage of this method is the use of adjustable parameters. The experimental data are usually recorded by thermocouples and gas-phase analyzer along the model adsorber. The intrusiveness and the influence of thermocouple thermal inertia may be a limitation for transient measurements such as adsorption processes [10].

Taking notice of these inconveniences, this work presents two high throughput devices based on infrared thermography for the estimation of adsorption heat via thin-layer approach, and of the propagation speed of thermal front in a millifluidic adsorption column. Simplified heat transfer model is then developed and the heat of adsorption is estimated using an inverse technique. The thin-layer approach allowed the prediction of the thermal front rate in the millifluidic adsorber, which is proportional to breakthrough time.

## 2 Thinlayer approach

The IR camera FLIR System A20M (Fig. 1: number 1) was coupled with an analytical balance METTLER TOLEDO XS204 DeltaRange (Fig. 1: number 2) to record the average temperature and mass variation of a thin-layer of adsorbent during $CO_2$ adsorptions and desorptions at room temperature. The sample mass variation is associated with adsorbed-phase evolution during $CO_2$ adsorption/desorption. The IR camera allows the detection of the thermal radiation (from 7.5 to 13 $\mu$m) coming from the adsorbent surface, and the temperature values can be directly measured through calibration parameters. A differential temperature measurement is recorded (sampling rate = 11 Hz) by using the same material as a reference to take into account the material emissivity and room temperature variation during the experiment. The precision balance measures the sample mass, and thanks to home-made Labview interface, the sample mass evolution is recorded (sampling rate = 1 Hz). Two filtering cartridges (made of insulating material) filled with a thin-layer of adsorbent (approximately 3 mm) are placed on the balance scale pan (Fig. 1: number 3) and one of them is connected with a gas injection system (Fig. 1: number 4). The injection system (multi-position valve, mass flow meters and 3-way valves) allows the switch on either $CO_2$ gas or $N_2$ gas (inert gas used to study $CO_2$ desorption) with a controlled injection time (home-made Labview interface). The 3-way valves are used to prevent excessive pressure between gas switching, thus the flow rate can be controlled without variation during adsorption/desorption cycles. The two mass flow metres Bronkhorst EL-FLOW are calibrated to take into account the gas temperature and density, thus allowing high accuracy (standard: ±0.5% Rd) measurement and control of gas flow rate. Moreover, thanks to controlled temperature of experiment room, the gas flow temperature is kept constant. Therefore, the temperature and flow rate of gas injected through thin-layer of adsorbent, consequently the related thermal exchanges, are mastered.

### 2.1 Simplified analysis of the rough signal through a lumped body model

As our experimental device leads to $CO_2$ adsorption on a thin-layer of adsorbent, we assumed that there is no temperature gradient in the layer thickness direction ($Bi \approx 10^{-4}$). Concerning the heat transfer between the

https://doi.org/10.1051/meca/2013080 Published online by Cambridge University Press

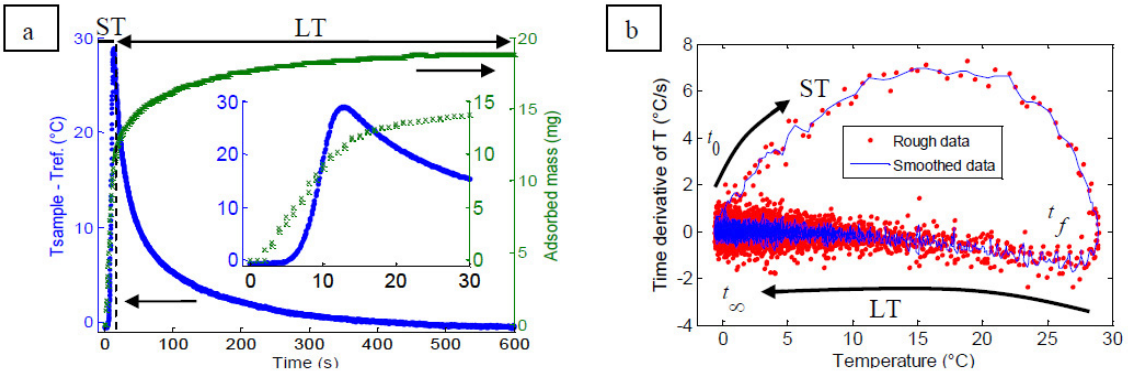



**Fig. 2.** (a) Recorded average temperature and adsorbed-phase evolution of adsorbent thin-layer during $CO_2$ adsorption. (b) Plot of time derivative of temperature versus temperature at every time step.

gas-phase and adsorbent grains, the internal resistance (adsorbent grain) is negligible compared to the external resistance (gas-phase) and the grain temperature is thus assumed as isothermal ($Bi \approx 10^{-5}$). Moreover, an average temperature of the thin-layer surface is recorded by the IR camera. The physical properties of the adsorbent are considered constant, $CO_2$ is considered as an ideal gas, and the accumulation of energy in the gas-phase is negligible [11]. With these assumptions, the thermal problem can be written as a lumped body model:

$$\underbrace{\frac{\mathrm{d}\left[\left(m_s Cp_s + m_s Cp_a q(t)\right)\overline{T}(t)\right]}{\mathrm{d}t}}_{\text{accumulation of heat}} = \underbrace{\phi(t)}_{\text{heat generated by the adsorption}} - \underbrace{h_o(t) A_{\text{eff}}\left(\overline{T}(t) - T_\infty\right)}_{\text{heat losses}} \quad (1)$$

with the initial condition at:

$$t = 0, \overline{T}(t) = T_\infty \quad (2)$$

where $m_s$ is the adsorbent mass (kg), $Cp_s$ the adsorbent heat capacity (J.kg$^{-1}$.K$^{-1}$), $Cp_a$ the adsorbed-phase heat capacity (J.mol$^{-1}$.K$^{-1}$), $q(t)$ the amount of molecules adsorbed (mol.kg$^{-1}$), $\overline{T}(t)$ the average temperature of thin-layer (K), $\phi(t)$ the adsorption heat flux (W), $h_0(t)$ the overall heat transfer coefficient (W.m$^{-2}$.K$^{-1}$), $A_{\text{eff}}$ the effective surface area (m$^2$) and $T_\infty$ the room temperature (K).

Considering a differential temperature measurement ($\overline{T}(t) = \overline{T}(t) - T_\infty$), equation (1) can be rewritten as follows:

$$\frac{\mathrm{d}\overline{T}(t)}{\mathrm{d}t} = \alpha(t) - H(t)\overline{T}(t) \quad (3)$$

with:

$$\alpha(t) = \frac{\phi(t)}{\left(m_s Cp_s + m_s Cp_a q(t)\right)} \quad (4)$$

$$H(t) = \frac{h_o(t) A_{\text{eff}}}{\left(m_s Cp_s + m_s Cp_a q(t)\right)} + \frac{m_s Cp_a}{\left(m_s Cp_s + m_s Cp_a q(t)\right)}\frac{\mathrm{d}q(t)}{\mathrm{d}t} \quad (5)\text{–}(6)$$

where $\alpha(t)$ and $H(t)$ are grouping parameters describing the heat source and heat losses respectively.

The presented lumped body model allowed a simplified analysis of the rough signal. In order to present the analysis, the recorded average temperature and adsorbed-phase evolution of an adsorbent thin-layer (about 3 mm) during $CO_2$ adsorption is shown in Figure 2a, and the plot of time derivative of temperature versus temperature at every adsorption time step is shown in Figure 2b. These data have been obtained with a commercial activated carbon ($m_s$ = 144 mg) which was subjected to continuous flow rate of pure $CO_2$ (40 ml.min$^{-1}$) during an injection time equals to 600 s.

Note: The smoothed data in Figure 2b were obtained by first-order finite difference method.

The results show two adsorption-time behaviors. In short-time adsorption period (ST), from $t_0$ = 0 s to $t_f$ = 14 s (see Fig. 2a), a high non-linear behavior between $\mathrm{d}\overline{T}(t)/\mathrm{d}t$ and $\overline{T}(t)$ was observed. In long-time adsorption period (LT), from $t_f$ = 14 s to $t_\infty$ = 600 s, there is a quasi-linear behavior between $\mathrm{d}\overline{T}(t)/\mathrm{d}t$ and $\overline{T}(t)$. Thanks to the lumped body model (Eq. (3)) we can propose an interpretation of results. At short-time, the non-linear behavior is related to the heat released during the adsorption process. This means that the heat source is on. However, at long-time, the results suggest that the energy released by the adsorption is negligible and that the heat source is off $\alpha\,(t_f \rightarrow t_\infty) = 0$. Therefore, a quasi-linear behavior is observed and can be interpreted as an evolution of the heat losses during $CO_2$ adsorption. This evolution is due to adsorbed-phase loading during $CO_2$ capture and to probable variation of overall heat transfer coefficient $h_0$ (see Eq. (5)).

The results suggest that the main release of heat is due to the first interactions between $CO_2$ molecules and adsorbent surface during the formation of a monolayer of adsorbed-phase. The adsorbates occupy the most energetically favorable positions and adsorbent-adsorbate interactions dominate. The evolution of adsorbed-phase after the short-time adsorption can be explained by the formation of a multilayer of adsorbate on adsorbent surface, which is intensified during the cooling of the adsorbent.

https://doi.org/10.1051/meca/2013080 Published online by Cambridge University Press

In the multilayer, the main interactions are adsorbate-adsorbate, which are less energetic, and the heat flux becomes negligible.

### 2.2 Heat of adsorption estimation

From the lumped body model (Eq. (3)), an inverse thermal model can be written as follows:

$$\phi(t) = \left[\frac{\mathrm{d}\overline{T}(t)}{\mathrm{d}t} + H(t)\overline{T}(t)\right](m_s Cp_s + m_s Cp_a q(t)) \quad (7)$$

The integral heat of adsorption could be estimated by the equations below:

$$\Delta H_{\mathrm{ads}} = \frac{Q}{N_{\mathrm{mol}}} \quad (\mathrm{J.mol^{-1}}) \quad (8)$$

with:

$$Q = \int_{t_i}^{t_f} \phi(t)\mathrm{d}t \quad \text{and} \quad N_{\mathrm{mol}} = m_s \int_{t_i}^{t_f} \frac{\mathrm{d}q(t)}{\mathrm{d}t}\mathrm{d}t \quad (9)$$

where $Q$ is the integral adsorption energy (J), $N_{\mathrm{mol}}$ the total amount of adsorbed $CO_2$ (mol), $\mathrm{d}q(t)/\mathrm{d}t$ the adsorption rate (mol.s$^{-1}$) and $t_i$, $t_f$ the time window where the heat source is active (s).

Therefore, to estimate the integral heat of adsorption, it is necessary at first, to estimate the heat flux $\phi(t)$. The main difficulty was thus the estimation of the heat losses. The heat losses were estimated at long-time adsorption, when the heat source is off. To strictly distinguish when the heat source is inactive, the coefficient of correlation ($\rho^{F_t}$) was studied [12]. This coefficient represents the normalized measure of the strength of linear relationship between variables (in our case, the average surface temperature of thin layer and its time derivative). If such correlation coefficient is close to $-1$, it is a proof that the thermal model has a linear behavior. It means that the heat source is off and the heat losses can be estimated.

Therefore, heat losses values ($H$) have been estimated within the range of $-0.99 > \rho^{F_t} > -1$. The maximum value of $H = 0.049$ s$^{-1}$ was used for posteriori estimations. After heat losses estimation, we can calculate the heat flux using equation (6). In order to estimate the integral heat of adsorption, the final step was the integration of heat flux curve from $t_i = 5$ to $t_f = 14$ s (for the estimation of integral adsorption energy $Q$) and then estimate, in the same time interval, the total amount of adsorbed $CO_2$ ($N_{\mathrm{mol}}$) from the adsorbed mass data. Finally, applying equation (7), $\Delta H_{\mathrm{ads}} = 28$ kj.mol$^{-1}$ was estimated for the interaction $CO_2$-adsorbent. The result is in good agreement with the values found in the literature for activated carbons: $\Delta H_{\mathrm{ads}} = (20\text{–}30)$ kj.mol$^{-1}$ [13–15]. For more information about our method see [16].

## 3 Millifluidic adsorption column: temperature field processing

High throughput studies of the influence of operating conditions (e.g. flow rate of injected gas into adsorption bed) on thermal behavior of adsorbers can be achieved by coupling a millifluidic adsorption column with an IR camera. The cylindrical adsorber is connected to a gas injection system and placed in an aluminum support (Fig. 3a). The milli-adsorber has internal diameter $d_2 = 5$ mm, external diameter $D_2 = 8$ mm, wall thickness $e_w = 1.5$ mm and adjustable length $L$. It was made in thermoplastic polymer (insulating material, $\lambda = 0.1\text{–}0.22$ W.m$^{-1}$.K$^{-1}$) to reduce the heat losses with surroundings and thus maximize the thermal signal received by the IR camera. The aluminum support (high thermal conductivity, $\lambda = 237$ W.m$^{-1}$.K$^{-1}$) was painted in black, to avoid reflections and to homogenize the surface emissivity. The $CO_2$ adsorption occurs thus in isoperibolic conditions, in other words, the temperature around the milli-adsorber is constant and uniform. The heat losses are thus mastered [17]. In order to illustrate some applications of the device, a commercial activated carbon (the same adsorbent used in thin-layer approach) was employed to run an experiment, which consisted in recording the temperature field during $CO_2$ adsorption for different flow rates (30, 40, 50, 60 and 70 ml.min$^{-1}$) of pure $CO_2$ injected into the adsorber. The milli-adsorber and its temperature field during $CO_2$ adsorption (flow rate = 40 ml.min$^{-1}$) at $t = 60$ s, is shown in Figure 3. The maximum observed temperatures were lower than in thin-layer approach. This can be explained by the semi-transparent behavior of adsorber wall in the infrared region. The IR signal detected by IR camera was thus weaker than in thin-layer approach. A thermal front with constant speed was observed during $CO_2$ capture. The analysis of thermal images and temperature evolutions (Fig. 4a), allowed the estimation of the propagation speed of the thermal front (TFR) in the milli-adsorber for each injected flow rate. Specifically, the TFR was estimated by the time it takes the thermal wave to pass through a section of the millifluidic adsorber.

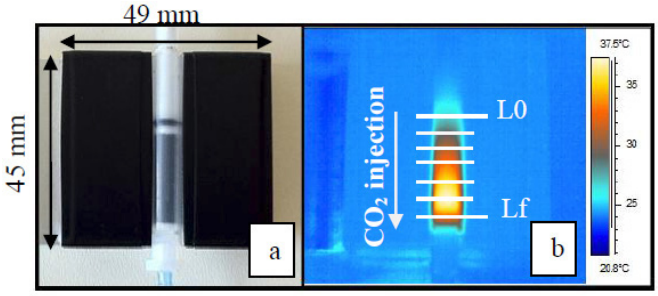



**Fig. 3.** (a) Millifluidic adsorption column. (b) Temperature field during $CO_2$ adsorption.

For a same flow rate traversing an identical volume of both thin-layer and millifluidic bed of adsorbent, a correlation between short-time adsorption (in thin-layer approach) and the thermal front rate (TFR) can be written as:

$$TFR = \frac{e_{\mathrm{fl}}\left(d_1/d_2\right)^2}{\tau_{\mathrm{ST}}} \quad (10)$$

where $e_{\mathrm{fl}}$ is the thin-layer thickness (mm), $\tau_{\mathrm{ST}}$ the breakthrough time (s) (temporal window of short-time

https://doi.org/10.1051/meca/2013080 Published online by Cambridge University Press

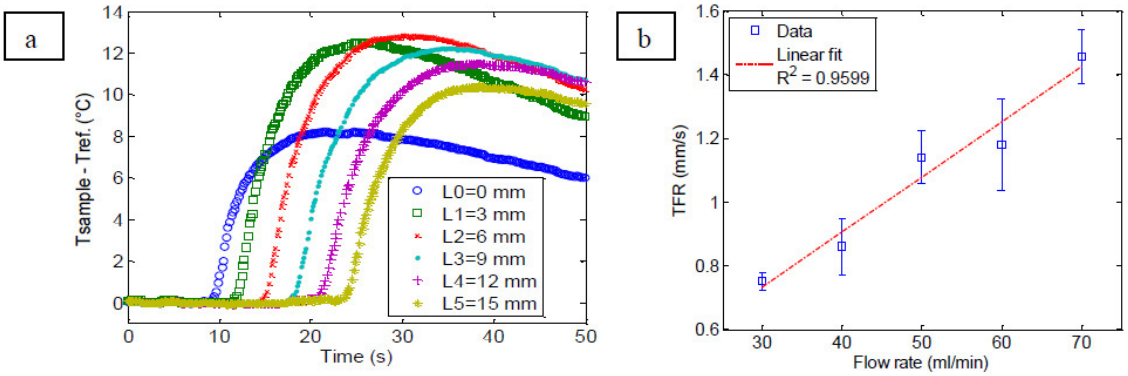



**Fig. 4.** (a) Average temperature in different sections of adsorber, from $L_0 = 0$ to $L_f = 15$ mm (see Fig. 3b) as a function of adsorption time. (b) Propagation speed of thermal front as a function of $CO_2$ flow rate.

adsorption, from $t_i$ to $t_f$) and $d_1$, $d_2$ the inner diameter of adsorption cup and millifluidic adsorber, respectively.

For example, the presented experiment in thin-layer approach ($CO_2$ injection of 40 ml.min$^{-1}$ through adsorbent thin-layer with $e_{fl} = 3$ mm) has led to a breakthrough time of $\tau_{ST} = 9$ s. Applying equation (9) to the found breakthrough time (with $e_{fl} = 3$ mm, $d_1 = 8$ mm and $d_2 = 5$ mm), a thermal front rate of $TFR = 0.85$ mm.s$^{-1}$ was calculated. This result is in good agreement with the estimated TFR in the millifluidic adsorption column for a same injection flow rate of 40 ml.min$^{-1}$: $TFR = 0.86$ mm.s$^{-1}$ (see Fig. 4b).

## 4 Conclusions and prospects

In order to study the mechanisms of $CO_2$ capture by solid adsorbents, we have developed two experimental devices based on IR thermography. The first device consists in coupling IR thermography and gravimetric techniques for simultaneous recording temperature and adsorbed mass evolution during $CO_2$ adsorption on adsorbent thin-layer. The second device consists in a millifluidic adsorption column in which the temperature field during adsorption process is also detected by IR thermography.

The thin-layer approach allows the identification and estimation of main parameters influencing $CO_2$ capture. These influent parameters, such as the heat of adsorption, can be used as key parameters for high throughput selection and overall comparison of materials. The millifluidic adsorber allows a high throughput study of operational conditions influencing temperature evolution and the estimation of thermal front rate, which is related to bed saturation. Moreover, a multi-scale analysis from thin-layer to adsorbent bed can be achieved.

The developed systems will be applied to perform systematic studies to better understand complex phenomena such as heat diffusion and transport.

Finally, thanks to its rapidity, the presented approach is interesting for preliminary design of processes to be used at industrial scale.

## References

[1] IPCC, Climate Change 2007: Synthesis Report, http://www.ipcc.ch/pdf/assessment-report/ar4/syr/ar4_syr.pdf
[2] J.D. Figueroa et al., Int J. Greenhouse Gas Control 2 (2008) 9–20
[3] Y. Liu et al., Micropor. Mesopor. Mater. 134 (2010) 16–21
[4] G.P. Knowles et al., Fuel Process. Technol. 86 (2005) 1435–1448
[5] R. Serna-Guerrero et al., Chem. Eng. J. 161 (2010) 173–181
[6] D.M. Ruthven, Principles of Adsorption and Adsorption Processes, Wiley, 1984
[7] F. Delage et al., Environ. Sci. Technol. 34 (2000) 4816–4821
[8] P. Pré et al., Environ. Sci. Technol. 36 (2002) 4681–4688
[9] L. Luo et al., Revue Générale de Thermique 35 (1996) 693–697
[10] A. Terzis et al., Influence of Thermocouple Thermal Inertia in Impingement Heat Transfer Experiments Using Transient Techniques, XXI Biannual Symposium on Measuring Techniques in Turbomachinery, Valencia, E, 2012
[11] P. Ozil et al., Chem. Eng. Sci. 33 (1978) 1233–1237
[12] J. Rodgers et al., Am. Stat. 42 (1988) 59–66
[13] S. Himeno et al., J. Chem. Eng. Data 50 (2005) 369–376
[14] K.T. Chue et al., Ind. Eng. Chem. Res. 34 (1995) 591–598
[15] C. Shen et al., Chem. Eng. J. 160 (2010) 398–407
[16] F. Benevides et al., Thermal effects of $CO_2$ Capture by Solid Adsorbents: Adsorption Heat Estimation by IR Image Processing, IPDO-2013, Albi-France, 2013
[17] C. Hany et al., Chem. Eng. J. 160 (2010) 814–822

https://doi.org/10.1051/meca/2013080 Published online by Cambridge University Press